ISSN (Print) 1226-1750
ISSN (Online) 2233-6656
Journal of Magnetics 24(3), 477-484 (2019) https://doi.org/10.4283/JMAG.2019.24.3.477

Electrical Resistivity and Demagnetization Characteristics of Salt-added Nd-Fe-B-type Magnet

M. S. Kang[1], K. M. Kim[1], H. W. Kwon[1]*, D. Wu[2], M. Yue[2], M. C. Kang[3], C. W. Yang[3], D. H. Kim[4], J. G. Lee[5] and J. H. Yu[5]

[1]*Pukyong National University, Busan 48513, Republic of Korea*
[2]*Beijing University of Technology, Beijing 100124, China*
[3]*Sungkyunkwan University, Suwon 16419, Republic of Korea*
[4]*Star-group Ind. Co., Daegu City 42714, Republic of Korea*
[5]*Korea Institute of Materials Science, Changwon 51508, Republic of Korea*

(Received 9 May 2019, Received in final form 3 September 2019, Accepted 11 September 2019)

Nd-Fe-B-type die-upset magnet with high electrical resistivity was fabricated by hot-deforming the mixture of melt-spun Nd-Fe-B-type flakes (MQU-F: $Nd_{13.6}Fe_{73.6}Co_{6.6}Ga_{0.6}B_{5.6}$) and Dy-containing salts: eutectic (DyF_3–LiF) salt mixture and DyF_3 single salt. Profound electrical resistivity enhancement was feasible in the Nd-Fe-B-type die-upset magnet by adding Dy-containing salts. More profound electrical resistivity enhancement was achieved in the magnet added with dielectric eutectic (DyF_3–LiF) salt mixture with respect to the magnet added with single DyF_3 salt. This was attributed to better electrical insulation between the flakes by forming more continuous coverage of the flake interface with the easily melted dielectric salt. Coercivity of the die-upset magnet was also profoundly enhanced by optimal addition of Dy-containing salts, and this was attributed to substitution of some Nd in the $Nd_2Fe_{14}B$-type grains near flake surface by Dy atoms from the added salt. Kerr microscopy revealed that for both the magnets with or without salt addition, formation of reverse domain initiated mostly inside the flake. Reversed domain started to form at higher reverse field for the magnet added with Dy-containing salt than for the magnet without salt addition. Practical demagnetization occurred largely by formation of new reverse domains at random places rather than enlargement of previously formed reverse domain for both the magnets with or without salt addition.

Keywords : Nd-Fe-B magnet, die-upset magnet, electrical resistivity, demagnetization process, Kerr microscopy

1. Introduction

Nd-Fe-B-type magnet is exclusively used as a rotor magnet in traction motor of hybrid electric vehicle (HEV) and electric vehicle (EV) by virtue of its most outstanding magnetic performance. The biggest plus point of the Nd-Fe-B-type magnet is, not to mention high remanence, hence having high energy product without comparison. The Nd-Fe-B-type magnet, however, has vulnerable point too due to its comparatively low Curie temperature. Curie temperature of the magnet is not sufficiently high and just above 310 ℃, and, to make matters worse, operating temperature of the magnet in traction motor is overly high (> 150 ℃). Improving the poor thermal stability of the magnet, in particular large temperature coefficient of coercivity (b) has, therefore, been a big challenge in utilizing this type magnet for a rotor magnet in traction motor of HEV and EV. Current standard approach around the problem is profoundly enhancing coercivity of the magnet by means of alloying and/or grain boundary diffusion using heavy rare earth (HRE) such as Dy, Tb [1-4]. Another option available as supplementary approach may be enhancing electrical resistivity of the magnet [5-10]. As the overly high operating temperature of the magnet in traction motor is due largely to eddy current generated in the magnet by varying magnetic field from slots of stator, enhancing electrical resistivity of the magnet can have especially positive effect on suppressing over-rise of operating temperature. The combo of enhancing electrical resistivity and coercivity of the magnet may, therefore, create an added synergy as a coping strategy for poor thermal stability of the magnet, hence burden of

*Corresponding author: Tel: +82-51-629-6362
Fax: +82-51-629-6353, e-mail: hwkwon@pknu.ac.kr

enhancing coercivity would, then, become less challenging. However, as the Nd-Fe-B-type magnet is, in essence, a metal alloy and highly conductive by nature, enhancing electrical resistivity in the magnet isn't as straightforward as one would think. In the present study, Nd-Fe-B-type die-upset magnet added with dielectric salt containing HRE was fabricated with the intention of simultaneously enhancing electrical resistivity and coercivity of the magnet. Demagnetization feature of the die-upset magnet added with the nonmagnetic salt was also investigated by observing the change of magnetic domain under reverse magnetic field.

2. Experimental

Nd-Fe-B-type die-upset magnet with high electrical resistivity was fabricated by die-upsetting technique: mixture of melt-spun Nd-Fe-B-type flakes (MQU-F: $Nd_{13.6}Fe_{73.6}Co_{6.6}Ga_{0.6}B_{5.6}$), flake size : 150-200 μm) and dielectric Dy-containing salts (particle size : ~1 μm) was first hot-pressed at 690 °C to obtain almost fully dense compact, and this magnetically isotropic compact was then die-upset at 735 °C in a vacuum with 75 % height reduction (strain = 0.75, strain rate = 1.25×10^{-2}/s) to prepare magnetically anisotropic magnet. As for dielectric Dy-containing salt, two types of salts were used; DyF_3 single salt and (DyF_3–LiF) binary salt mixture. The DyF_3 – LiF binary salt system has an eutectic reaction in it, and composition of the binary salt mixture used was eutectic composition of (25 mol% DyF_3–75 mol% LiF) with eutectic temperature of as low as approximately 700 °C [11]. As the die-upsetting temperature used was higher than melting point of the eutectic salt mix, the added binary salt mixture became liquid during die-upsetting. Thus, easier penetration of the dielectric salt into the interface of flakes, hence more profound enhancement of electrical resistivity, was expected in the magnet added with the eutectic (DyF_3–LiF) salt mixture with respect to the magnet added with single DyF_3 salt, which had high melting point (1360 °C) and existed as solid throughout entire processing. Electrical resistivity of the magnets was measured by means of a Four-Point probe. Magnetic properties were measured using combination of SQUID (max. field = 5 T) and VSM. Microstructure observation and composition analysis were conducted by SEM(EDX), TEM and EPMA. Demagnetization characteristics of the die-upset magnets were investigated using a Kerr microscopy. Sample (1.6 × 4.7 × 2.2 mm) for Kerr microscopy was cut from the die-upset magnet, and magnetic domain change under reverse field was observed on the 1.6 × 4.7 mm plane parallel to the easy axis. Easy axis on the plane was along 1.6 mm axis (demagnetizing factor $N_D = 0.35$). The sample was fully magnetized by applying 10 T pulse field along the easy axis, and then domain structure change under reverse field was observed. Strength of reverse field presented in the text was effective reverse field compensated using demagnetizing factor of 0.35.

3. Results and Discussion

Figure 1 shows dependence of electrical resistivity of the $Nd_{13.6}Fe_{73.6}Co_{6.6}Ga_{0.6}B_{5.6}$ die-upset magnet on the amount of added salts. Effectiveness of adding the eutectic (DyF_3–LiF) salt mixture and single DyF_3 salt on electrical resistivity of the die-upset magnet was also compared in Fig. 1. Addition of the salts led to enhancement of electrical resistivity of the magnet, and the magnet added with eutectic (DyF_3–LiF) salt mixture exhibited consistently higher electrical resistivity with respect to the magnet added with single DyF_3 salt. The magnet added with more than 6 vol% of eutectic (DyF_3–LiF) salt mixture had high electrical resistivity over 400 μΩ·cm, which was almost 2.5 times as high electrical resistivity as that of the magnet without salt addition. The drastic enhancement of electrical resistivity achieved in the magnet with addition of eutectic (DyF_3–LiF) salt mixture was attributed to continuously distributed thin dielectric layer of the salt mixture along the interface between flakes. As the die-upsetting of the magnet was carried out at 735 °C, which was far higher than melting point (~ 700 °C) of the added eutectic (DyF_3–LiF) salt mixture, the added salt became liquid and more easily penetrated into the interface of flakes. Thus homogeneous and continuous dielectric layer had more effectively insulated the flakes as shown in Fig. 2(a). While, the added single DyF_3 salt with melting point (1360 °C) still existed as solid during the die-upsetting,

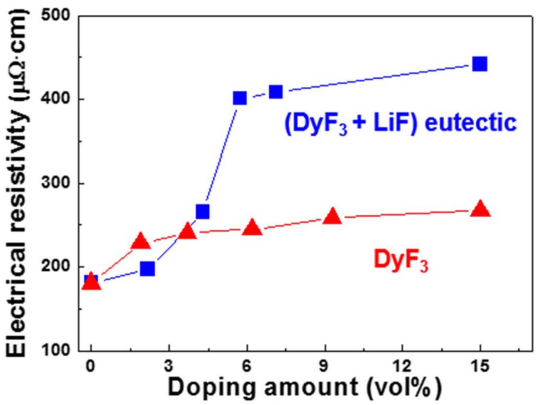

Fig. 1. (Color online) Dependence of electrical resistivity of the $Nd_{13.6}Fe_{73.6}Co_{6.6}Ga_{0.6}B_{5.6}$ die-upset magnet on the amount of added salts.

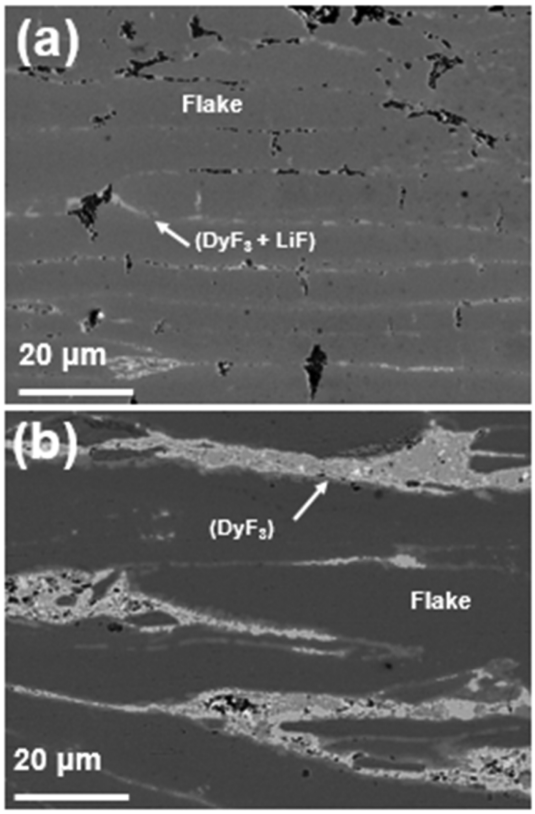

Fig. 2. SEM (BSE) micrographs of the $Nd_{13.6}Fe_{73.6}Co_{6.6}Ga_{0.6}B_{5.6}$ die-upset magnet added with (a) 7 vol% eutectic (DyF_3–LiF) salt mixture and (b) 6 vol% DyF_3 single salt.

thus the added dielectric salt was more likely to be agglomerated and less continuously distributed between the flakes (Fig. 2(b). This was responsible for the less profound enhancement of electrical resistivity in the magnet with addition of DyF_3 single salt compared to the magnet with addition of eutectic (DyF_3–LiF) salt mixture.

Figure 3 shows variations of magnetic performance of the die-upset magnet with varying the amount of added eutectic (DyF_3–LiF) salt mixture or DyF_3 single salt. Addition of both eutectic and single salts caused significant enhancement of coercivity of the die-upset magnet, and it was notable that more remarkable coercivity enhancement was achieved in the magnet added with eutectic (DyF_3–LiF) salt mixture with respect to the magnet added with DyF_3 single salt. Coercivity enhancement in the magnet added with salts was caused by the substitution of some Nd in the flakes by Dy atoms from the added salt. DyF_3 in the added salt had first reacted with Nd atoms from the flake: Nd atoms preferably combined with fluorine to form NdF_3 and to release Dy atoms. This was verified by Dy distribution analysis by EPMA as shown in Fig. 4. Flake interface was the region which was originally occupied by added salt of DyF_3 or (DyF_3–LiF). As can be

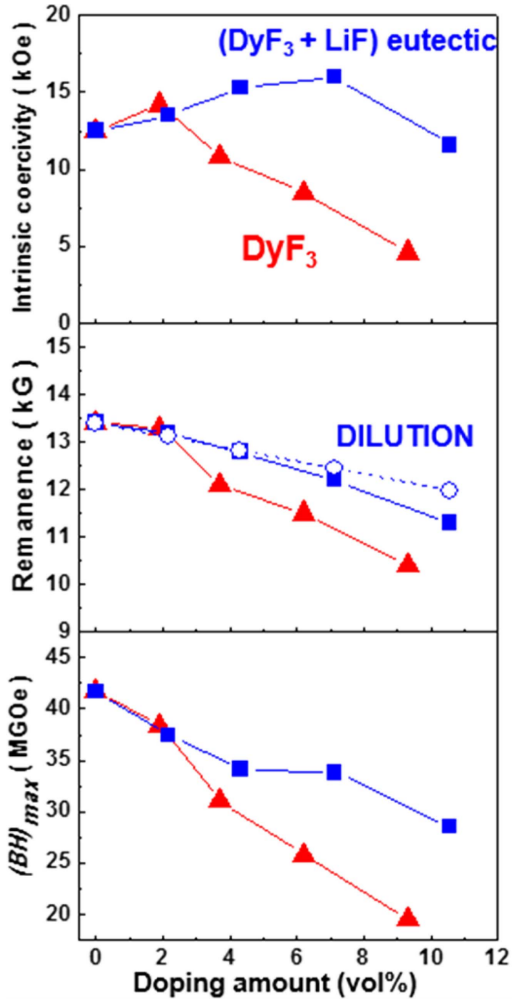

Fig. 3. (Color online) Variations of magnetic performance of the salt-added $Nd_{13.6}Fe_{73.6}Co_{6.6}Ga_{0.6}B_{5.6}$ die-upset magnet as a function of vol% of added salts.

seen in Fig. 4, Dy element mapping showed that Dy atoms were hardly found in the flake interface region which was originally occupied by the Dy-containing salt mixture. On the other hand, Nd element mapping clearly showed that Nd atoms were found to exist in the flake interface region which was originally occupied by added Dy-containing salt. The flake interface was the region where there was no Nd atoms. This observation clearly indicated that some Nd atoms from flakes had migrated into the (DyF_3–LiF) salt mixture region and substituted Dy atoms in some DyF_3 to form NdF_3 to release some Dy atoms. The released Dy atoms were believed to diffuse into surface of the flakes. As the two thermal processes of hot-pressing and die-upsetting were performed for very brief time period, diffusion of the Dy atoms into the flake probably had occurred only near surface of the flake. This was verified by observing the distribution profile of Dy

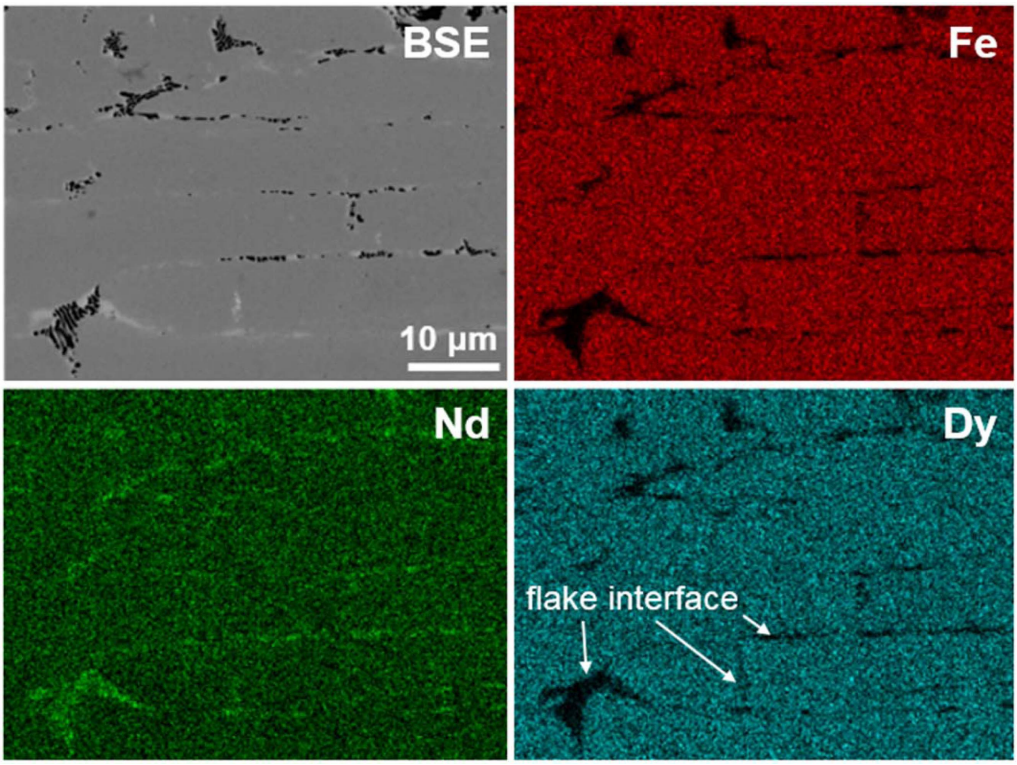

Fig. 4. (Color online) BSE photo and elemental mapping images of some elements in the $Nd_{13.6}Fe_{73.6}Co_{6.6}Ga_{0.6}B_{5.6}$ die-upset magnet doped with 7 vol% of eutectic (DyF_3–LiF) salt mixture.

atoms across the flake interface filled with (DyF_3–LiF) salt mixture or DyF_3 single salt. As can be seen in Fig. 5, Dy atoms were found to exist not only in the flake interface region but also near surface of the flake, indicating that some Dy atoms migrated into the surface of flake from the added Dy-containing salts. Diffusion depth of Dy into

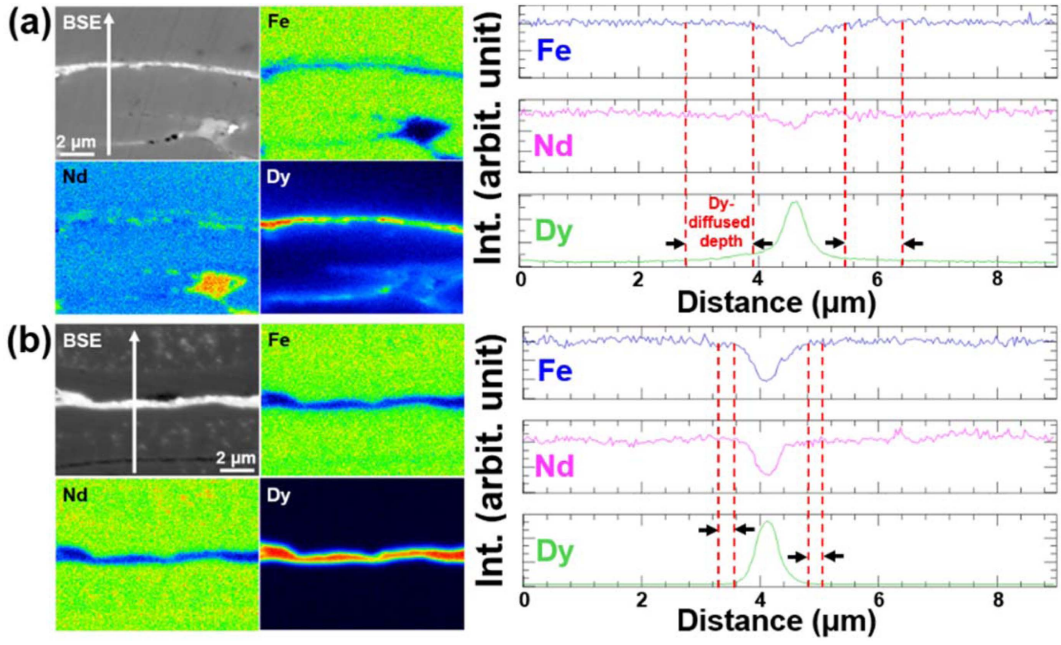

Fig. 5. (Color online) EPMA line analysis profile of Dy element in the $Nd_{13.6}Fe_{73.6}Co_{6.6}Ga_{0.6}B_{5.6}$ die-upset magnet added with (a) 7 vol% of (DyF_3–LiF) salt mixture and (b) 6 vol% DyF_3 single salt.

the flake surface was deeper (around 1.2 μm) in the magnet added with (DyF_3–LiF) salt mixture with respect to the magnet added with DyF_3 single salt (far narrower diffusion depth of around 0.3 μm). As the added eutectic (DyF_3–LiF) salt mixture was liquid during die-upsetting, Dy diffusion into flakes had occurred more swiftly and actively in the magnet added with eutectic salt compared to the magnet added with DyF_3 single salt, which still existed as solid during die-upsetting. More remarkable coercivity enhancement in the magnet added with eutectic (DyF_3–LiF) salt mixture with respect to the magnet added with DyF_3 single salt was, therefore, attributed to the formation of thicker Dy-diffused shell in the surface of flake. It would seem that observations of Dy atom distribution by Dy atom mapping in Fig. 4 and Dy atom distribution profile in Fig. 5 conflict with each other: while Dy atoms were hardly found in the flake interface region in Fig. 4, their presence was observed in Fig. 5. This conflict may be simply due to poor resolution of x-ray element mapping in SEM(EDX). Nd atoms migrated from flakes substituted some of Dy atoms in the added salts, and there was still lot of Dy atoms in the flake interface, which had not yet been substituted. Presence of Dy atoms in the flake interface, which had not yet been substituted, was observed in a more precise analysis of Dy atom by EPMA(WDX). In the analysis of element distribution, analysis of Li atoms was not performed because of difficulty due to its very light nature. Fluorine was known to exist still in the flake interface as state of DyF_3 or NdF_3 in the salt added magnet and to be almost insoluble in the $Nd_2Fe_{14}B$-type matrix phase. Presence of fluorine was also known to exert little influence on the magnetic performance of the magnet [12].

We couldn't help wondering if the Dy atoms had substituted some of Nd atoms only in the grain boundaries or in both the grain boundary and $Nd_2Fe_{14}B$-type grain interior near surface. Fig. 6 shows microstructure and distribution of Dy atoms in the magnet added with eutectic (DyF_3–LiF) salt mixture. Seeing the presence of Dy atoms, the observed region was believed to be near flake surface contacting with the Dy-containing salts. First, point analyses on four different regions were performed and Dy content in the regions were summarized in Fig. 6(a). Among the four regions, 1, 2, and 4 regions were found to be $Nd_2Fe_{14}B$-type grains, and region 3 was Nd-rich grain boundary phase. It appeared that the $Nd_2Fe_{14}B$-type grains contained some Dy atoms, although grain 1 appeared to contain no Dy atoms. This indicated that some Nd atoms in the $Nd_2Fe_{14}B$-type grains near surface of the flake contacting with eutectic (DyF_3–LiF) salt mixture had been substituted by Dy atoms from the salt to become $(Nd,Dy)_2Fe_{14}B$-type grains. Dy atoms were also found to substitute some of Nd atoms in the Nd-rich grain boundaries in the Dy-diffused shell near flake surface.

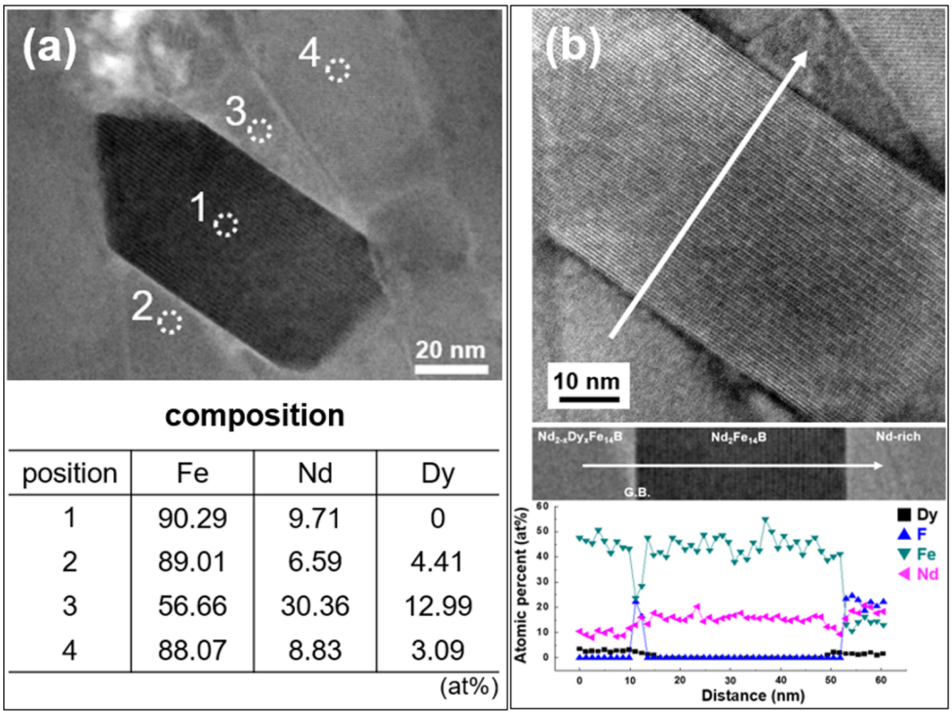

Fig. 6. (Color online) (a) TEM micrograph showing grain structure and composition in the flake contacting with eutectic (DyF_3–LiF) salt mixture region, (b) Distribution of Dy atoms in the $Nd_{13.6}Fe_{73.6}Co_{6.6}Ga_{0.6}B_{5.6}$ die-upset magnet across grains 2, 1, and 3.

Line analysis across the $Nd_2Fe_{14}B$-type grains and Nd-rich grain boundary phase also confirmed that some Nd atoms in both the $Nd_2Fe_{14}B$-type grains and grain boundaries had been substituted by Dy atoms as shown in Fig. 6(b). As the $Nd_2Fe_{14}B$-type grains near flake surface had been modified to Dy-substituted $(Nd,Dy)_2Fe_{14}B$-type grains, the anisotropy field of the grains probably had been enhanced due to the Dy-substitution [13, 14]. Therefore, formation of reverse domain and/or domain wall movement under reverse applied field was significantly suppressed, hence enhancing coercivity. Remanence of the die-upset magnets added with salts decreased with increasing amount of added salts, and, needless to say, this was attributed to dilution of magnetization by addition of the non-magnetic salt. It was noted, however, that remanence of the magnet added with eutectic (DyF_3–LiF) salt mixture was measurably lower than that expected from the magnetization dilution due to addition of non-magnetic salt. This was attributed to the reduced development of texture caused by the presence of liquid salt during die-upsetting. The liquid salt may have acted as lubricant between flakes during die-upsetting, thus the flakes readily glided outwards during die-upsetting. The $Nd_2Fe_{14}B$-type grains in flake were, then, subjected to reduced pressure, leading to poor texture development. Remanence was more radically reduced in the magnet added with DyF_3 single salt. The added DyF_3 salt existed as agglomerated large solid packet during die-upsetting, and the large solid packets may have interfered with developing texture, leading to poor texture. Fig. 7 shows temperature dependence of remanence and intrinsic coercivity of the die-upset magnet added with eutectic (DyF_3–LiF) salt mixture or DyF_3 single salt. On investigating magnetic performance of the die-upset magnet, magnets that exhibited peak coercivity were selected: ones added with 7 vol% of (DyF_3–LiF) salt mixture and 2 vol% DyF_3 single salt, respectively (Fig. 3). Temperature dependence of remanence (a) and intrinsic coercivity (b) of the die-

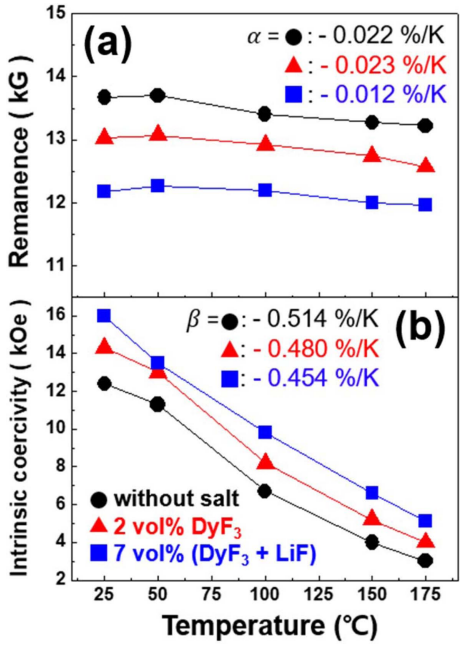

Fig. 7. (Color online) Temperature dependence of (a) remanence and (b) intrinsic coercivity of the $Nd_{13.6}Fe_{73.6}Co_{6.6}Ga_{0.6}B_{5.6}$ die-upset magnet added with 7 vol% of (DyF_3–LiF) salt mixture and 2 vol% DyF_3 single salt.

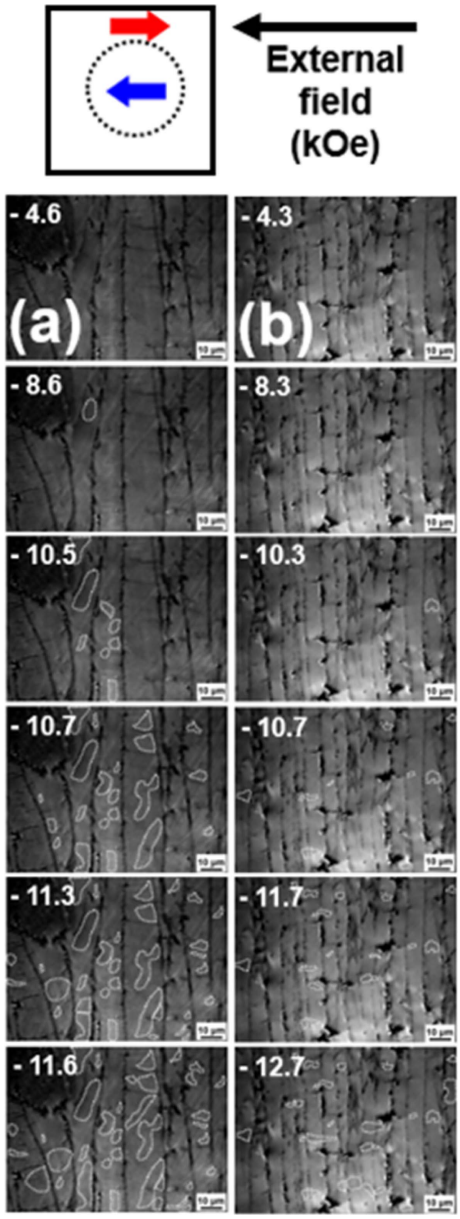

Fig. 8. (Color online) Kerr images showing change of magnetic domain structure under reverse field for the fully magnetized $Nd_{13.6}Fe_{73.6}Co_{6.6}Ga_{0.6}B_{5.6}$ die-upset magnets with and without 2 vol% DyF_3 salt.

upset magnet added with the salts appeared to be more or less similar with those of the magnet without salt addition.

Figure 8 shows change of magnetic domain structure under reverse field for the fully magnetized magnets observed by Kerr microscopy, showing demagnetization process in the die-upset magnet with and without addition of Dy-containing salt. For observation of magnetic domain structure change during demagnetization process in the die-upset magnet added with Dy-containing salt, the magnet added with DyF_3 single salt was selected. On sample preparation for Kerr microscopy, the added eutectic (DyF_3–LiF) salt in the magnet was very brittle and deep grooves were easily produced along the flake interface. As these grooves might influence magnetic domain structure change during demagnetization, magnetic domain structure change during demagnetization in the die-upset magnet added with Dy-containing salt was observed using the magnet added with DyF_3 single salt. The added DyF_3 single salt was less brittle and appearance of deep grooves along the flake interface was noticeably suppressed. As can be seen in Fig. 8, practical demagnetization started to take place at reverse field of approximately 8.6 kOe for the magnet without salt addition, while it started at much higher reverse field of approximately 10.3 kOe for the magnet added with Dy-containing salt. It appeared that for both the magnets with or without salt addition, formation of reverse domain initiated mostly inside the flake. As increasing reverse external field, practical demagnetization proceeded largely by formation of new reverse domains at random places, some of the previously formed reverse domains seemed to enlarge though. This was the case for both the magnets with and without the salt addition. At the reverse field near coercivity (12.4 kOe) of the magnet without salt addition, good portion of area (or volume) had been demagnetized, while majority of area still stayed in unreversed state and only small portion of area had been reversed in the magnet added with DyF_3 salt at the reverse field. At further higher reverse field near coercivity (14 kOe) of the magnet added with DyF_3 salt, area of reversed domain in the magnet had been further increased. The demagnetization process observed by the domain structure change was in good sync with demagnetization curve of the magnets with or without salt addition shown in Fig. 9.

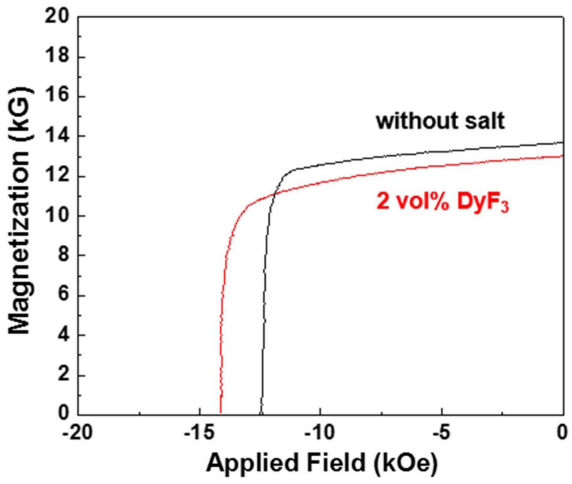

Fig. 9. (Color online) Demagnetization curves of the $Nd_{13.6}Fe_{73.6}Co_{6.6}Ga_{0.6}B_{5.6}$ die-upset magnet with and without the addition of 2 vol% DyF_3 single salt.

4. Conclusion

Profound electrical resistivity enhancement was feasible in the Nd-Fe-B-type die-upset magnet by adding Dy-containing salts, and more profound enhancement was achieved in the magnet added with dielectric eutectic (DyF_3–LiF) salt mixture with respect to the magnet added with single DyF_3 salt. This was attributed to better electrical insulation between the flakes by forming more continuous coverage of the flake interface with the easily melting dielectric salt. Coercivity of the die-upset magnet was also profoundly enhanced by optimal addition of Dy-containing salts, and this was attributed to substitution of some Nd in the $Nd_2Fe_{14}B$-type grains near flake surface by Dy atoms from the added salt. More profound coercivity enhancement was achieved in the magnet added with dielectric eutectic (DyF_3–LiF) salt mixture with respect to the magnet added with single DyF_3 salt. As the added eutectic (DyF_3–LiF) salt was liquid during die-upsetting, more quick and active diffusion of Dy into flakes was possible. Kerr microscopy revealed that for both the magnets with or without salt addition the formation of reverse domain initiated mostly inside the flake. Reverse domain started to form at higher reverse field for the magnet added with Dy-containing salt than for the magnet without salt addition. Practical demagnetization occurred largely by formation of new reverse domains at random places rather than enlargement of previously formed reverse domain for both the magnets with or without salt addition.

Acknowledgement

The authors gratefully acknowledge that the present work was supported by a Research Grant of Pukyong National University, Republic of Korea (year 2019).

References

[1] H. Nakamura, K. Hirota, M. Shimao, T. Minowa, and M. Honshima, IEEE Trans. Magn. **41**, 3844 (2005).
[2] K. Hirota, H. Nakamura, T. Minowa, and M. Honshima, IEEE Trans. Magn. **42**, 2909 (2006).
[3] J. Y. Kim, H. W. Kwon, J. G. Lee, and J. H. Yu, IEEE Trans. Magn. **52**, 2100904 (2016).
[4] K. M. Kim, J. Y. Kim, H. W. Kwon, D. H. Kim, J. G. Lee, and J. H. Yu, AIP Adv. **7**, 056232 (2017).
[5] Y. Aoyama, K. Miyata, and K. Ohashi, IEEE Trans. Magn. **41**, 3792 (2005).
[6] M. Komuro, Y. Satsu, Y. Enomoto, and H. Koharagi, Appl. Phys. Lett. **91**, 102503 (2007).
[7] M. Komuro and Y. Satsu, J. Appl. Phys. **103**, 07E142 (2008).
[8] M. Marinescu, A. M. Gabay, J. F. Liu, and G. C. Hadjipanayis, J. Appl. Phys. **105**, 07A711-1 (2009).
[9] S. Sawatzki, I. Dirba, L. Schultz, and O. Gutfleisch, J. Appl. Phys. **114**, 133902 (2013).
[10] S. S. Nair, J. Wang, and L. Chen, IEEE Trans. Energy. Conv. **32**, 414 (2017).
[11] P. P. Fedorov, Russian J. Inorg. Chem. **44**, 1703 (1999).
[12] S. Sawatzki, I. Dirba, H. Wendrock, L. Schultz, and O. Gutfleisch, J. Magn. Magn. Mater. **358**, 163 (2014).
[13] J. F. Herbst, Rev. Mod. Phys. **63**, 819 (1991).
[14] G. Yan, P. J. McGuiness, J. P. G. Farr, and I. R. Harris, J. Alloys Compd. **491**, L20-L24 (2010).